POLITECNICO DI TORINO
Repository ISTITUZIONALE

A robust MPC approach for the rebalancing of mobility on demand systems

(Article begins on next page)

18 April 2024

A Robust MPC Approach for the Rebalancing of Mobility on Demand Systems

Giuseppe C. Calafiore[a,b], Christian Bongiorno[a], Alessandro Rizzo[a,*]

[a]Dipartimento di Elettronica e Telecomunicazioni - Politecnico di Torino - Torino - Italy
[b]IEIIT-CNR Torino, Italy

Abstract

A control-oriented model for mobility-on-demand systems is here proposed. The system is first described through dynamical stochastic state-space equations, and then suitably simplified in order to obtain a control-oriented model, on which two control strategies based on Model Predictive Control are designed. The former aims at keeping the expected value of the number vehicles parked in stations within prescribed bounds; the latter specifically accounts for stochastic fluctuations about the expected value. The model includes the possibility of weighting the control effort, leading to control solutions that may trade off efficiency and cost. The models and control strategies are validated over a dataset of logged trips of ToBike, the bike-sharing systems in the city of Turin, Italy.

Keywords:

Mobility on Demand, Bike-sharing, Rebalancing, Traffic Models, Nonlinear Models, Data Analysis, Model Predictive Control

*[*]Corresponding Author
Email address: alessandro.rizzo@polito.it (Alessandro Rizzo)
URL: http://staff.polito.it/alessandro.rizzo (Alessandro Rizzo)

1. Introduction

Mobility-on-Demand (MOD) systems are becoming pervasive in cities of any size. As of December 2016, bike- and car-sharing programs had been adopted by more than 1,000 cities worldwide [1]. As of July 2017, Car2Go, the largest car-sharing company in the world, has 2,500,000 registered users and a fleet of nearly 14,000 vehicles in 26 locations in North America, Europe, and Asia [2].

The concept behind a MOD system is straightforward: a user requires a vehicle, picks it up from a designated location, executes the trip, drops off the vehicle at her/his destination. MOD systems can be station-based, with vehicles parked at fixed locations (stations), or floating, with vehicles parked with no constraints, at the user's wish.

As required to all service providers, MOD systems should be designed to meet the customer demand, which is extremely heterogeneous due to several factors, such as the time of the day, the season, commuting patterns, up-hill or down-hill stations (for bikes) [3, 4, 5]. The impossibility of meeting the customer demand is usually caused by a lack of vehicles at some locations and a corresponding surplus of vehicles somewhere else. This issue can be mitigated through the implementation of repositioning policies, also called *rebalancing.* Rebalancing strategies are typically obtained as the solution of suitable optimization problems. In bike-sharing systems, most of the works in the literature assume that one or more trucks are available to redistribute bikes over the city, aiming at maximizing the system performance while keeping the repositioning effort at a minimum. In car-sharing systems, rebalancing is operated on a single-vehicle basis by operators [6].

Rebalancing is often executed during time periods where traffic is low, especially at night. This activity, called *static rebalancing,* assumes that vehicles are

not used by customers during repositioning operations, or that their use is negligible with respect to the rebalancing flows. In bike-sharing systems, repositioning is usually executed by trucks able to displace high volumes of bikes, even within relatively long distances [7, 8, 9, 10, 11, 12, 12, 13, 14, 15, 16]. *Dynamic repositioning,* on the other hand, assumes that customers are traveling while rebalancing operations occur, and the effects of such travels are not negligible. This kind of repositioning is usually performed with smaller vehicles and/or over shorter distances [17, 18, 19, 20]. Users may also be involved in system rebalancing through incentives [21]. For example, in Paris, Velib+ offers rewards to people moving bikes up-hill [22].

Optimization algorithms informing repositioning strategies are based on suitable models of the MOD system. Several modeling techniques have been proposed in the literature, mostly based on statistical and data-driven approaches, to account for the stochasticity of the system under exam [23, 24, 25, 26, 27]. Most of these works, however, rely on models with limited analytical tractability, due to the lack of specific dynamical equations.

In this paper, a novel control-oriented model for a station-based MOD system is proposed, extending preliminary results presented in [28]. In its general formulation, the system is described by a dynamical model with stochastic state variables in discrete time. The model quantifies vehicle flows between different locations and accounts for stochasticity in customer demand and traveling times. Hence, it is used to derive two MPC-based techniques [29]: first, a linear and time-invariant approximation of the model is derived. Such a model is used to control the expected values of the state variables, representing the expected quantity of vehicles at each station. Then, interval analysis is leveraged to develop a robust

control strategy on the stochastic model, thus accounting for the fluctuations about the expected values.

The design of the mentioned control strategies yields constrained optimization problems, with the objective of maintaining the number of vehicles within prescribed bounds at each location. As a solution to these problems, vehicle flows that tend to rebalance the system are derived. These flows can then be used to devise incentive-based strategies, or to set up rebalancing campaigns operated by trucks or other transportation means.

Even though the proposed approach is conceived for station-based systems, it can be effectively applied to free-floating systems, via a suitable tessellation of the operational space. Location-based rebalancing can be also useful when stations are close to each other, and users can effortlessly move through groups of stations to seek for suitable pick-up or drop-off locations. This is the case, for example, of the ToBike bike-sharing systems, located in the city of Turin (Italy), on which the proposed approach is validated using one year of logged user trip data.

This paper extends preliminary results presented in [28] along several directions: *i)* the dynamical model is better formalized, and a more in-depth theoretical treatment is offered; *ii)* the control of the expected value is expanded and includes now a detailed study of steady-state conditions; *iii)* a robust control strategy based on interval modeling is devised; *iv)* model and control validation are performed on a real dataset of one year of logged trips provided by ToBike.

The paper is structured as follows. In Section 2 the modeling rationale, model parameters, nomenclature, and modeling assumptions toward the realization of a control-oriented model are given. Section 3 introduces the control-oriented model, studying in detail the dynamics of the expected value of the state variables and the

4

steady-state conditions. In Section 4, two MPC-based control strategies, first on the expected value of the space variables, and then, on robust bounds of the state variables, are proposed. The ToBike MOD system and the dataset adopted for validation, along with relevant data analysis techniques are described in Section 5. Section 6 comprehensively validates our model and assesses its performance, using the ToBike dataset. Conclusions are finally drawn in Section 7.

2. Control- and simulation-oriented models of the MOD system

A MOD system is here modeled as a network composed by nodes, representing the vehicle stations, and links between nodes, representing the vehicle routes. The set $\mathscr{S}$ of station nodes is composed by N stations, and the set $\mathscr{L}$ is composed by N^2 links between any two station nodes in $\mathscr{S}$. A link (i,j) between departure station i and destination station j does not necessarily represent a specific physical route, but rather the ensemble of all routes that are typically traveled by customers moving from i to j.

The generic link (i,j) is characterized by its state $v_{ij}(t)$, representing the cardinality of the set $\mathscr{V}_{ij}(t)$ of all the vehicles *en route* from i to j at time t, and by the (random) fraction $\tilde{q}_{ij}(t,\delta) \in [0,1]$ of the $v_{ij}(t)$ vehicles that reach their destination j within the time interval $(t, t+\delta]$.

The generic node i is characterized by its state $z_i(t)$, denoting the number of vehicles parked (and hence available for pick up) at station i at time t, and by the instantaneous mean rate $\mu_i(t) \in \mathbb{R}^+$ of random service requests that arrive at station i at time t. Analogously, $1/\mu_i(t)$ describes the mean of the random inter-arrival time of service requests at station i. The station throughput $\lambda_i(t)$ is instead the mean rate at which vehicles depart from station i. In reality, it always holds

5

that $\lambda_i(t) \leq \mu_i(t)$, since not all the service requests may be fulfilled, due to the
fact that there may exist station-empty periods in which no vehicles are available
at the station, and hence no departure is possible from the station, even if demand
from customers exists. This issue is further discussed in Section 2.1.4.

If a customer request is generated at station i at time t, and if station i has a
vehicle available, then the customer picks up that vehicle and starts a trip towards
a destination station j. The selection of the destination is modeled via a set of
(possibly time-varying) *routing probabilities*, i.e., it is assumed that at time t and
for each station i, there exist probabilities $p_{ij}(t) \in \mathbb{R}^+$, with $\sum_j p_{ij}(t) = 1$, such
that a generic customer departing from i chooses destination j with probability
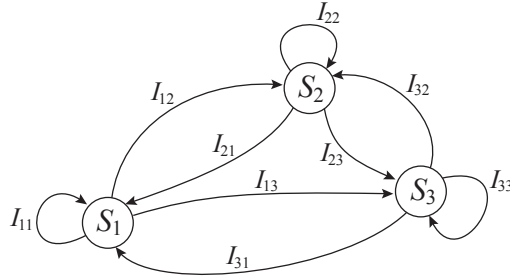$p_{ij}(t)$.

Figure 1: Example of network modeling a MOD system with three stations S_1, S_2, S_3, and corresponding itinerary links I_{ij}.

2.1. Simplifying assumptions for a "control-oriented" model

A real-life MOD system is hardly representable by a simple mathematical
model. For one thing, any stochastic representation of, say, the transit times or
of the customer requests, is only an approximation of reality. Also, a key aspect
in station-based MOD systems is that a station state $z_i(t)$ may reach its physical

6

limits, that is, $z_i(t)$ may be equal to zero (empty state) or to $c_i^{\max}$ (full state), where $c_i^{\max}$ is the maximum capacity of the station (typically, the number of physical slots available for parking the vehicles in station i). When $z_i(t) = 0$, customer requests at the i-th station cannot be fulfilled and must be turned down. Similarly, when $z_i(t) = c_i^{\max}$, vehicles arriving at station i at time t are unable to park their vehicles, and must therefore wait, or be diverted to some other stations that have available parking slots. The two issues just mentioned are indeed a manifestation of a common problem in MOD systems known as "station imbalance," a situation in which certain stations are over-requested as departure stations, and thus quickly become empty, and other stations are over-requested as destination stations, and thus quickly become full. Strong imbalance severely affects the usability (and the economic profitability) of the system.

Clearly, it is possible to build a sophisticated model that tries to mimic as close as possible the behavior of the real system. This is what is usually called a *simulation model*, which is needed for testing policies and assessing the system performance via simulations. Such a model is a proxy of reality, and it may be used in place of reality, whenever this is needed. The model presented in this paper, on the other hand, has a different goal: to develop a *control model*, that is, a model whose primary purpose is to help in the design of control strategies (e.g., rebalancing policies) for the system. A good control model should be simple enough to allow for the effective synthesis of the control law, although this may come at the expense of approximations. In the end, however, the performance of the control law should be tested and evaluated on the real system, or on a proxy of it (i.e., the simulation model).

With this in mind, the main simplifying assumptions used to construct the

control-oriented model of the MOD system are introduced in the following.

2.1.1. Piece-wise constant parameters

The model discussed so far has time-varying parameters, matching the fact that rates, routing probabilities and transit times of a real-world system are likely not constant over time. However, dealing with continuously time-varying parameters is impractical for our purposes of system optimization. Previous analyses performed on logged service data suggest that system parameters can be conveniently approximated as piece-wise constant functions [23, 24], where each constant part corresponds to a subset of the day. Motivated by this observation, constant parameters over each given period are here considered.

2.1.2. Exponential inter-departure times

Departures from each station i follow a counting process with instantaneous rate $\lambda_i(t)$. For simplicity, it is specifically assumed that they form a Poisson process of rate $\lambda_i(t)$, although this latter assumption is not critical for our developments. Assuming that each vehicle departing from i at time t chooses its destination j with probability $p_{ij}(t)$ implies that vehicles departing from i with destination j at time t also follow a Poisson process with rate $p_{ij}(t)\lambda_i(t)$.

2.1.3. Densities for link arrival proportions

As previously discussed, the transit of vehicles through the (i, j) link is modeled by assuming that, at each given t and given δ, only a (random) fraction $\tilde{q}_{ij}(t, \delta) \in [0, 1]$ of the $v_{ij}(t)$ vehicles reach their destination j within the time interval $(t, t + \delta]$. Letting

$$q_{ij}(t, \delta) \doteq \mathrm{E}\left\{\tilde{q}_{ij}(t, \delta)\right\} \in [0, 1],$$

8

159 it is assumed that $\tilde{q}_{ij}(t, \delta)$ is statistically independent from $v_{ij}(t)$. The characteri-

160 zation of $\tilde{q}_{ij}(t, \delta)$ should be done via a specific statistical analysis of log data from

161 the real (or simulated) system. If the average transit times $\tau_{ij}(t)$ are estimated for

162 each link (i, j), for instance, then one may choose the expected proportion as

163 $q_{ij}(t, \delta) = 1 - \mathrm{e}^{-\delta/\tau_{ij}(t)}$, or simply as $q_{ij}(t, \delta) = \delta/\tau_{ij}(t)$, for $\delta \leq \tau_{ij}(t)$.

164 *2.1.4. No blocking*

165   It is assumed, for the purpose of the control model, that stations have unlimited

166 capacity, i.e., $c_i^{\max} = +\infty$, $\forall i$. Also, it is fictiously assumed that customer demand

167 is always satisfied. The motivation for these assumptions is explained in the fol-

168 lowing. In reality, a station state $z_i(t)$ remains bounded in $[0, c_i^{\max}]$ at all times.

169 When one of the two limits in the interval is attained, the station is "blocked", in

170 the sense that no operations can occur until an event (i.e., a departure for a full

171 station or arrival for an empty station) that takes the station state back within the

172 prescribed capacity limits happens. Reproducing the "blocking" condition in our

173 control-oriented model would prevent us from developing a time-driven model

174 and hinder the tractability of the model. Hence, we here admit that variables

175 $z_i(t)$ are allowed to go beyond the boundaries, while penalizing out-of-boundary

176 behavior is penalized in the control design phase. Thus, the control action is rein-

177 forced until the imbalance situation is compensated. Letting $z_i(t) > c_i^{\max}$ implies,

178 in practice, to assume that there are always enough parking slots at the station,

179 and letting $z_i(t) < 0$ implies to assume that there are always enough vehicles at

180 the stations; this just implies that unavailable vehicles are borrowed from some-

181 where in order to satisfy the demand. The rebalancing control policy, however,

182 will be designed to minimize such out-of-boundary situations.

9

3. The MOD control model

Under the assumptions of Section 2.1, the following quantities are defined:

- Δ is the time period during which the system parameters are assumed to be constant, as discussed in Section 2.1.1.

- n_h is a convenient positive integer number used to divide the whole simulation time T in equally spaced time intervals of duration $\delta = T/n_h$.

- $d_{ij}(t+\delta)$ is the number of vehicles driven by users that depart from i with destination j in the time interval $(t, t+\delta]$. According to the assumption in Section 2.1.2, $d_{ij}(t+\delta)$ has a Poisson probability mass

$$\text{Prob}\{d_{ij}(t+\delta) = k\} = \frac{1}{k!}(p_{ij}(t)\lambda_i(t)\delta)^k e^{-p_{ij}(t)\lambda_i(t)\delta},$$

$$\text{for } k = 0, 1, \ldots. \quad (1)$$

- $r_{ij}(t)$ is the number of "control" vehicles (i.e., vehicles used for rebalancing purposes) that are moved from i to j as dictated by the rebalancing control strategy. From a modeling point of view, these are considered to be "injected" in the (i,j) link during the interval $(t, t+\delta]$. Contrary to $d_{ij}(t+\delta)$, $r_{ij}(t)$ is a deterministic quantity that is determined by the control algorithm at time t. It is assumed that δ is sufficiently small with respect to the average link transit times τ_{ij}, so that there is a (practically) zero probability that any of the $d_{ij}(t+\delta)$ or of the $r_{ij}(t)$ vehicles reaches its destination by time $t+\delta$.

- $a_{ij}(t+\delta)$ is the number of vehicles, among the ones in $\mathcal{V}_{ij}(t)$, that reach the j-th station by time $t+\delta$. According to the assumption in Section 2.1.3, the

10

count $a_{ij}(t+\delta)$ can be written equivalently in terms of the *random proportion* $\tilde{q}_{ij}(t,\delta)$ as

$$a_{ij}(t+\delta) = \tilde{q}_{ij}(t,\delta)v_{ij}(t), \qquad (2)$$

where $\tilde{q}_{ij}(t,\delta)$ is a random parameter with expected value $q_{ij}(t,\delta)$. Equation (2) simply states that the number of vehicles in $\mathcal{V}_{ij}(t)$ that reach the j-th station by time $t+\delta$ is a (random) fraction of the whole number of vehicles in $\mathcal{V}_{ij}(t)$, and this fraction is, on average, equal to $q_{ij}(t,\delta)$. We observe that the quantity $a_{ij}(t+\delta)$ is implicitly allowed to be real valued.

Table 1 summarizes the notation of main variables used in this paper.

The discrete-time equations that regulate the system behavior can now be written. For $i,j = 1,\ldots,N$, straightforward conservation arguments yield

$$
\begin{aligned}
v_{ij}(t+\delta) &= v_{ij}(t) - a_{ij}(t+\delta) + d_{ij}(t+\delta) + r_{ij}(t) \\
z_j(t+\delta) &= z_j(t) + \sum_i a_{ij}(t+\delta) - \sum_h \left(d_{jh}(t+\delta) + r_{jh}(t) \right).
\end{aligned}
$$

The following equations are obtained using (2):

$$
\begin{aligned}
v_{ij}(t+\delta) &= (1-\tilde{q}_{ij}(t,\delta))v_{ij}(t) + \\
&\qquad\qquad +d_{ij}(t+\delta) + r_{ij}(t) \qquad (3) \\
z_j(t+\delta) &= z_j(t) + \sum_i \tilde{q}_{ij}(t,\delta)v_{ij}(t) + \\
&\qquad\qquad - \sum_h \left(d_{jh}(t+\delta) + r_{jh}(t) \right). \qquad (4)
\end{aligned}
$$

The system above is a linear, discrete-time, stochastic one in the z_j and v_{ij} state variables, with stochastic inputs given by the d_{ij} departures, and control inputs given by the rebalancing departures r_{ij}. Given initial conditions, Eqs. (3)-(4) can be used to propagate forward in time the (random) system states. In the following,

11

Variable	Description
N	Number of stations
t	Discrete time index
Δ	Time interval in which system parameters are assumed to be constant
δ	Sampling interval
n_h	Time horizon used for optimization in MPC
$v_{ij}(t)$	Number of vehicles *en route* from station i to station j at time t
$\tilde{q}_{ij}(t,\delta)$	Fraction of $v_{ij}(t)$ vehicles that reach station j within the interval $(t,t+\delta)$
$q_{ij}(t,\delta)$	Average value of $\tilde{q}_{ij}(t,\delta)$
$a_{ij}(t+\delta)$	Number of vehicles that reach station j from station i by time $t+\delta$
$\mu_i(t)$	Instantaneous mean rate of service request at station i at time t
$\lambda_i(t)$	Instantaneous mean rate of station i throughput
$p_{ij}(t)$	Routing probability from station i to station j at time t
$c_i^{\min}, c_i^{\max}$	Bounds for the desired number of vehicles available at station i
$r_{ij}(t)$	Number of "control" (rebalancing) vehicles to be displaced from station i to station j at time t

Table 1: Nomenclature of the main variables used in the paper.

the dynamics of the expected value of the model state variables will be derived and used to design the first MPC-based controller.

4. MPC-based rebalancing

4.1. The expected state dynamics

Observing that $\sum_h d_{jh}(t+\delta)$ is Poisson with parameter $\sum_h p_{jh}\lambda_j\delta = \lambda_j\delta$, denoting expected quantities with an overbar (i.e., $\bar{v}_{ij}(t) \doteq \mathrm{E}\{v_{ij}(t)\}$, $\bar{z}_j(t) \doteq$

12

$E\{z_j(t)\}$, etc.), and recalling that $\tilde{q}_{ij}(t,\delta)$ and $v_{ij}(t)$ are assumed to be statistically independent, the evolution of the expected value of the state equations in (3)-(4) can be written as

$$
\begin{aligned}
\bar{v}_{ij}(t+\delta) &= (1 - q_{ij}(t,\delta))\bar{v}_{ij}(t) + \\
&\qquad + p_{ij}(t)\lambda_i(t)\delta + r_{ij}(t) \quad (5) \\
\bar{z}_j(t+\delta) &= \bar{z}_j(t) + \sum_i q_{ij}(t,\delta)\bar{v}_{ij}(t) + \\
&\qquad - \lambda_j(t)\delta - \sum_h r_{jh}(t). \quad (6)
\end{aligned}
$$

Equations (5)-(6) constitute a linear, discrete-time, deterministic dynamical system in the expected state variables $\bar{z}_j(t)$ and $\bar{v}_{ij}(t)$, with inputs given by the mean departure rates $\lambda_i(t)$, and control inputs given by the rebalancing departures $r_{ij}(t)$.

4.2. Steady-state behavior

Assume that the rebalancing inputs are constant, i.e., $r_{ij}(t) = r_{ij}$, $\forall t$, and that the system parameters p_{ij}, q_{ij}, and λ_j, $i,j = 1,\ldots,N$, remain constant. In such case, the following equations hold:

$$
\begin{aligned}
\bar{v}_{ij}(t+\delta) &= (1 - q_{ij}(\delta))\bar{v}_{ij}(t) + p_{ij}\lambda_i\delta + r_{ij} \quad (7) \\
\bar{z}_j(t+\delta) &= \bar{z}_j(t) + \sum_i q_{ij}(\delta)\bar{v}_{ij}(t) - \lambda_j\delta - \sum_h r_{jh}. \quad (8)
\end{aligned}
$$

Since $1 - q_{ij}(\delta) < 1$, the discrete time recursion (7) is asymptotically stable, and has a constant input term equal to $p_{ij}\lambda_i\delta + r_{ij}$. Therefore, $\bar{v}_{ij}(t+k\delta)$ approaches a steady-state value for $k \to \infty$, independently from the initial condition $\bar{v}_{ij}(t)$, and this value is

$$
\bar{v}_{ij}^{(ss)} = \frac{p_{ij}\lambda_i\delta + r_{ij}}{q_{ij}(\delta)}. \quad (9)
$$

13

Plugging the steady-state value (9) into (8), a steady-state for $\bar{z}_j^{(\mathrm{ss})}$ exists when

$$\bar{z}_j^{(\mathrm{ss})} = \bar{z}_j^{(\mathrm{ss})} + \delta \sum_i p_{ij}\lambda_i - \lambda_j\delta + \sum_i r_{ij} - \sum_h r_{jh}.$$

This steady state condition is satisfied if the following flow equilibrium holds for all $j = 1,\ldots,N$:

$$\delta \sum_i p_{ij}\lambda_i + \sum_i r_{ij} = \lambda_j + \sum_h r_{jh}. \tag{10}$$

Since (8) is a pure discrete-time integrator, the actual steady-state value depends on the initial conditions and on the transient of $\bar{v}_{ij}(t + k\delta)$. Incidentally, it can be observed that if $\delta \ll \Delta$, since the system parameters p_{ij} and λ_j, $i,j = 1,\ldots,N$, remain constant within an interval of duration Δ, it may be assumed that $\bar{v}_{ij}(t+k\delta)$ and $\bar{z}_j(t + k\delta)$ will rapidly attain their steady-state value.

4.3. Control of the expected value

The adopted cost function is the total weighted rebalancing effort over the considered time horizon

$$J_T = \sum_{k=0}^{n_h-1} \|\mathrm{vec}(\mathbf{W} \circ \mathbf{R}(t+k\delta))\|_1,$$

where $\mathbf{R}(t + k\delta)$ is the matrix containing in row i and column j the rebalancing departures $r_{ij}(t + k\delta)$, $\mathbf{W} \in \mathbb{R}^{N,N}$ is a weight matrix with nonnegative elements, the operator $\mathrm{vec}(\cdot)$ indicates the operation of vectorization of a matrix, the operator "$\circ$" indicates the Hadamard product, and $\|\cdot\|_1$ indicates the 1-norm of a vector. The weight matrix can be used to specify the relative cost of rebalancing between different pairs of stations, due for example to high displacement time, level of traffic, steep routes, etc. For simplicity and to enhance readability, and without loss of

generality, in this work we set $\mathbf{W}$ as the all-one matrix and we omit the vectorization notation, so that we define $\|\mathbf{R}(t+k\delta)\|_1 \doteq \|\text{vec}(\mathbf{R}(t+k\delta))\|_1$. The control goal is to maintain the expected states $\bar{z}_j(t+k\delta)$ within given limits $[c_j^{\min}, c_j^{\max}]$, at all times, while minimizing the rebalancing effort. Letting

$$\mathscr{R} \doteq \{\mathbf{R} \in \mathbb{R}^{N,N} : \mathbf{R} \geq 0, \text{ and } R_{ii} = 0, \ i = 1,\ldots,N\},$$

the following optimization problem is solved:

$$\min_{\mathbf{R}(t),\ldots,\mathbf{R}(t+(n_h-1)\delta)\in\mathscr{R}} \sum_{k=0}^{n_h-1} \|\mathbf{R}(t+k\delta)\|_1$$

$$\text{s.t.:} \quad \bar{z}_j(t+k\delta) \in [c_j^{\min}, c_j^{\max}],$$

$$\text{for} \quad j = 1,\ldots,N, \text{ and } k = 1,\ldots,n_h,$$

where $\bar{z}_j(t+k\delta)$ is given by the recursion in (5)-(6), initialized with given initial conditions $\bar{z}_j(t)$, $\bar{v}_{ij}(t)$, $i,j = 1,\ldots,N$.

Imposing strict feasibility for the state limits $\bar{z}_j(t+k\delta) \in [c_j^{\min}, c_j^{\max}]$ may result in infeasibility, or in a too high rebalancing effort for most of the possible scenarios. A more flexible approach is therefore to consider a trade-off between rebalancing effort and constraint satisfaction, by introducing slack variables $s_j(t+k\delta)$. Slack variables are used in this case to allow a certain degree of violation of the station capacity constraint against a mitigation of the control effort. The state constraint is firstly rewritten as

$$\left| \bar{z}_j(t+k\delta) - \frac{c_j^{\max} + c_j^{\min}}{2} \right| \leq \frac{c_j^{\max} - c_j^{\min}}{2},$$

15

and then the problem is relaxed to

$$
\min \sum_{k=0}^{n_h-1} \sum_j s_j(t+k\delta) + \gamma \|\mathbf{R}(t+k\delta)\|_1
$$

$$
\text{s.t.:} \left| \bar{z}_j(t+k\delta) - \frac{c_j^{\max} + c_j^{\min}}{2} \right| \leq \frac{c_j^{\max} - c_j^{\min}}{2} + s_j(t+k\delta),
$$

$$
s_j(t+\delta) \geq 0, \dots, s_j(t+n_h\delta) \geq 0,
$$

$$
\text{for } j = 1, \dots, N, \text{ and } k = 1, \dots, n_h,
$$

$$
\mathbf{R}(t), \dots, \mathbf{R}(t+(n_h-1)\delta) \in \mathscr{R},
$$

(11)

where $\gamma \geq 0$ is a tunable trade-off parameter between the rebalancing effort and satisfaction of the capacity constraints. Variables $s_j(t+k\delta)$ represent the amount of allowed capacity violation at the j-th station at time $t+k\delta$. Ideally, the optimization problem should lead to a sharp satisfaction of the capacity constraint, hence, the minimized cost function should entail slack variables equal to zero. However, some scenarios might allow a much reduced control effort, if some of the capacity constraints are relaxed. In this case, the optimization algorithm would attain a value of the objective function such that some of the slack variables settle to a nonzero value, implying that the capacity constraint is violated by an amount equal to such a value. The trivial constraints on the nonnegativity of the slack variables and on the feasibility of the control actions complete the definition of the problem.

4.4. MPC based on robust interval modeling

Although the control procedure illustrated in Section 4.3 is an efficient way to control the expected values of the state variables, the stochastic nature of the system may lead to fluctuations that take the system dynamics out of the desired

16

behavior during specific realizations. This issue is here mitigated through the introduction of a robust control scheme based on interval analysis.

The stochastic information on $d_{ij}(t,\delta)$ in (1) can be used to obtain an interval of probabilistic confidence on this parameter, and hence it is possible to use interval analysis to unroll in time a confidence tube to bound the state of the dynamical system (3)-(4). Then, MPC will be applied to control the resulting dynamics. The obtained control scheme will guarantee the attainment of the control objective with the desired confidence level.

Fixing a probability level η, quantities $d_{ij}^{\min}(t,\delta)$ and $d_{ij}^{\max}(t,\delta)$ denote the extremes of confidence intervals of probability η for the random variable $d_{ij}(t,\delta)$. Due to the linearity of (3)-(4) in $d_{ij}(t,\delta)$, two conservative bounds within which state variables $v_{ij}(t)$ and $z_j(t)$ will be contained with probability η can be easily obtained. Denoting these bounds with $v_{ij}^{\min}(t)$, $v_{ij}^{\max}(t)$, $z_j^{\min}(t)$, and $z_j^{\max}(t)$, their dynamics is described by

$$
\begin{aligned}
v_{ij}^{\min}(t+\delta) &= (1-\tilde{q}_{ij}(t,\delta))v_{ij}^{\min}(t)+ \\
&\quad +d_{ij}^{\min}(t+\delta)+r_{ij}(t) \qquad (12) \\
z_j^{\min}(t+\delta) &= z_j^{\min}(t)+\sum_i \tilde{q}_{ij}(t,\delta)v_{ij}^{\min}(t)+ \\
&\quad -\sum_h \left(d_{jh}^{\max}(t+\delta)+r_{jh}(t)\right) \qquad (13)
\end{aligned}
$$

and

$$
\begin{aligned}
v_{ij}^{\max}(t+\delta) &= (1-\tilde{q}_{ij}(t,\delta))v_{ij}^{\max}(t)+ \\
&\quad +d_{ij}^{\max}(t+\delta)+r_{ij}(t) \qquad (14) \\
z_j^{\max}(t+\delta) &= z_j^{\max}(t)+\sum_i \tilde{q}_{ij}(t,\delta)v_{ij}^{\max}(t)+ \\
&\quad -\sum_h \left(d_{jh}^{\min}(t+\delta)+r_{jh}(t)\right). \qquad (15)
\end{aligned}
$$

17

The optimization problem that implements the MPC strategy is analogous to
that of Section 4.3, with the difference that the algorithm considers now a larger
set of constraints to impose that the two extremes of fluctuations are bounded
between two given capacity limits:

$$
\min_{\mathbf{R}(t),\ldots,\mathbf{R}(t+(n_h-1)\delta)\in\mathscr{R}} \quad \sum_{k=0}^{n_h-1} \|\mathbf{R}(t+k\delta)\|_1
$$

$$
\text{s.t.:} \quad z_j^{\min}(t+k\delta) \in [c_j^{\min}, c_j^{\max}],
$$

$$
z_j^{\max}(t+k\delta) \in [c_j^{\min}, c_j^{\max}],
$$

$$
\text{for } j=1,\ldots,N, \text{ and } k=1,\ldots,n_h.
$$

Similarly to Section 4.3, two sets of slack variables, denoted as $s_j^{\max}(t)$ and $s_j^{\min}(t)$, are used to establish a trade-off between feasibility, rebalancing effort, and constraint satisfaction. The optimization problem is therefore relaxed to

$$
\min \sum_{k=0}^{n_h-1} \sum_j [s_j^{\max}(t+k\delta) + s_j^{\min}(t+k\delta)] + \gamma\|\mathbf{R}(t+k\delta)\|_1
$$

$$
\text{s.t.:} \left| z_j^{\max}(t+k\delta) - \frac{c_j^{\max} + c_j^{\min}}{2} \right| \le \frac{c_j^{\max} - c_j^{\min}}{2} + s_j^{\max}(t+k\delta),
$$

$$
\left| z_j^{\min}(t+k\delta) - \frac{c_j^{\max} + c_j^{\min}}{2} \right| \le \frac{c_j^{\max} - c_j^{\min}}{2} + s_j^{\min}(t+k\delta), \tag{16}
$$

$$
s_j^{\max}(t+\delta) \ge 0,\ldots,s_j^{\max}(t+n_h\delta) \ge 0,
$$

$$
s_j^{\min}(t+\delta) \ge 0,\ldots,s_j^{\min}(t+n_h\delta) \ge 0,
$$

$$
\text{for } j=1,\ldots,N, \text{ and } k=1,\ldots,n_h,
$$

$$
\mathbf{R}(t),\ldots,R(t+(n_h-1)\delta) \in \mathscr{R},
$$

where the constraints have the same meaning of Eq. 11.

5. ToBike system description, data analysis, and parameter identification

ToBike has been Turin's (Italy) bike-sharing system since 2010. It comprises more than 160 stations and 2000 bikes. Stations contain a variable number of docking slots. About 8000 trips per day are executed by more than 20,000 customers within an area of approximately 300 square kilometers. No reservation system is available, but users can use a mobile app to check the number of bikes and docking slots available at a given station. A user that wishes to travel can pick up an available bike at any station, cycle toward a destination station and dock it to an available docking slot. Bike stations are very dense in the urban territory, especially around the city center. Thus, in most of the cases, the availability of bikes is much efficiently and representatively computed over groups of stations, rather than on single ones. Toward the design of an effective control algorithm, stations have therefore been grouped in clusters, according to their geographic location. Clustering has been performed via a k-means algorithm [30] and a Voronoi tessellation, partitioning the city territory in $N = 10$ groups of stations, based on the Euclidean distance between them. Such a distance is evaluated on the azimuthal equidistant projection [31] of the geographical coordinates, with the azimuth set on the geometric center of the stations. A similar partition strategy can be used to apply our modeling and control approach to free-floating systems, i.e., systems where vehicles are not obliged to be picked up and dropped off at stations and balancing should be pursued over urban zones to be determined according to given criteria [32].
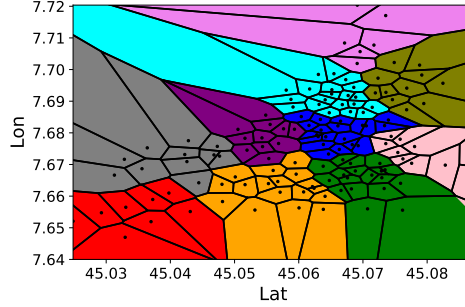
19

Figure 2: Voronoi tessellation of the urban territory for vehicle rebalancing strategies, obtained through our clustering algorithm. Each point represents a station. The color code indicates the station groups obtained with a *k*-means algorithm.

After the grouping procedure, each selected location contains a different number of stations. For simulation purposes, the initial number of bikes in each location and the location capacity constraints $c_j^{\min}$, $c_j^{\max}$ are set up to be proportional to the number of stations that each group contains, denoted as N_j, $j = 1 \ldots 10$. Table 2 summarizes such values for the selected locations.

Data analysis confirms the intuition that bike trips have a strong seasonality along the day, week, and year time-scales, and that there exist recurrent time periods with a travel activity close to zero. A significant and dynamically rich dataset is therefore obtained by filtering out from the database the time periods in which usage is extremely low and can be approximated to zero. In particular, all the trips occurred in 2015 during all workdays from 8AM to 8PM are considered, excluding January, February (when bikes are almost not used due to the low temperatures), and August (holiday month in Italy for the majority of people). Furthermore, all the rebalancing operations made by ToBike operators are removed from the database.

A piece-wise constant identification of the parameters is performed, with a

20

location	N_j	$z_j(0)$	$c_j^{\min}$	$c_j^{\max}$
1	8	80	40	120
2	19	190	95	285
3	18	180	90	270
4	6	60	30	90
5	17	170	85	255
6	11	110	55	165
7	20	200	100	300
8	11	110	55	165
9	10	100	50	150
10	11	110	55	165

Table 2: Summary of location parameters: number of stations after the clustering procedure (N_j), initial number of bikes at the beginning of each simulation ($z_j(0)$), lower and upper capacity bounds ($c_j^{\min}$, $c_j^{\max}$).

312 time period of $\Delta = 1$ hour. Specifically, $\lambda_i(t)$ is estimated as the average number
313 of bikes per minute that leave location i in the hourly time-window that contains
314 t; $p_{ij}(t)$ is estimated as the fraction of bikes that leave i and arrive in j in the
315 hourly time-window that contains t. Data analysis leads to the observation that
316 travel durations are not affected by the time of the day. Thus, the dependency on t
317 of $\tilde{q}_{ij}(t, \delta)$ can be neglected, and according to section 2.1.3, such quantity can be
318 estimated as $\tilde{q}_{ij}(\delta) = 1 - e^{-\delta/\tau_{ij}}$, where τ_{ij} is the average transit time over the link
319 (i, j). This simplification would likely not apply to car sharing systems, where car
320 trip durations are heavily affected by traffic conditions. More details and alternate
321 approaches on the identification of the system parameters can be found in our

previous works [23, 24].

Due to the mentioned choices in the data analysis phase, a day-long simulation consists of twelve instances of simulation of Eqs. (3)-(4), where parameters are considered to vary in an hourly piece-wise constant fashion and the initial value of state variables in each simulation phase after the first one is set equal to the final value of the preceding one. Figure 3(a) shows the outcome of a Monte Carlo simulation campaign executed over 100 daily independent simulations, illustrating the distribution of the percentage variation of the number of bikes with respect to the initial value $z_i(0)$, in absence of control action, i.e., $r_{ij}(t) \equiv 0, \forall i, j, t$. It can be observed that the system dynamics tends to evolve toward imbalance conditions, with some locations that tend to fill in at the expense of others, which tend to become empty. Figure 3(c) illustrates more in detail this condition, by plotting the trend of the number of bikes in location 4 over a day, that is, $z_4(t)$, highlighting the trend for this location to fill up as long as time progresses.

In order to assess the performance of the proposed control algorithms, a stress test is first carried out in open loop, by proportionally increasing the original $\lambda_i(t)$ estimated from trip data to the value $\alpha \lambda_i(t)$, where the stress factor $\alpha > 1$, for all stations at all times, simulates a perturbation upon the usual operational conditions. Since this is an open loop test, rebalancing inputs are considered null at any time, that is, $r_{ij}(t) \equiv 0, \forall i, j, t$.

In the proposed simulation, the stochastic equations (3)-(4) are simulated selecting $\alpha = 4$ and generating departures according to Eq. (1). The application of such increased departure rates yields an important imbalance on all locations, as can be observed by comparing Figs. 3(a) and 3(b). It can be observed that even the application of smaller values of the stress factor α to departure rates im-

22

plies important imbalance throughout the stations. To this aim, Fig. 3(d) plots the trend of the *global imbalance parameter* f_E as a function of the stress factor α. Such a global imbalance parameter is defined as the average number of bikes, per time-step δ, that exceeds the prescribed capacity bounds at each location. More specifically, it is computed as $f_E = \sum_{k=0}^{n_h-1} \sum_j s_j (t + k\delta)/n_h$. It can be observed that important imbalances are revealed for values of α slightly greater than the unity, to then grow rapidly as the stress factor α increases.

6. Results

In this section, we present extensive numerical results to assess the performance of the proposed rebalancing strategies. The main performance parameters here analyzed are summarized in Table 3.

Variable	Description
γ	Trade-off between rebalancing accuracy and control effort
η	Confidence interval for the attainment of the robust control objective
f_E	Random variable expressing the global imbalance per time step
f_R	Random variable expressing the global control effort per time step
$\mathscr{R}_{\text{link}}$	Random variable expressing the total control effort per link
$\mathscr{D}_{\text{link}}$	Random variable expressing the total traffic intensity per link

Table 3: Nomenclature of the main performance parameters used in the paper.

6.1. Control of the expected values

The first set of numerical experiments concerns the application of the MPC-based control of the expected values of the state variables, as described in Sec-

tion 4.3. Notably, the optimization program (11) is solved to generate the control inputs, which are in turn applied to Eqs. (3)-(4) to simulate the dynamical system response. Fixing a time horizon of n_h time units, the whole control sequence $\{\mathbf{R}_{ij}(t), \mathbf{R}_{ij}(t+\delta), \cdots, \mathbf{R}_{ij}(t+n_h\delta)\}$ is generated solving (11)[1]. Then, only the control action $R_{ij}(t)$ is applied to the simulator in Eqs. (3)-(4). At each time step, the simulator selects the number of bikes $d_{ij}(t)$ moving from i to j according to a Poisson process with expected value $\lambda_i(t)p_{ij}(t)$ plus the control operation $R_{ij}(t)$. The number of bikes arriving from i to j are selected via a probabilistic rounding [33] of $q_{ij}(\delta)v_{ij}(t-1)$. Here and henceforth, the whole simulation time is fixed to $T = 12$ hours, and the time-step to $\delta = 15$ minutes, unless differently specified. The MPC control strategy is executed over a shrinking observation window with duration $T = 12$ hours, and with a prediction horizon $n_h = 48$ time units, that is, 12 hours.

An extensive Monte Carlo simulation campaign is executed to validate the proposed approach, achieving satisfactory results. One hundred independent simulations are performed, randomized in the realizations of the vehicle departures, starting from the initial conditions of Table 2. Figure 4 exemplifies the obtained results, illustrating the trend of the occupancy of two locations (variables z_4 and z_7) over a 12 hours interval, from 8AM to 8PM, in uncontrolled and controlled situations, respectively. The two locations have different spatial characteristics: location 4 is peripheral, whereas location 7 is central. As can be observed from the figure, in uncontrolled mode location 4 tends to become empty at the beginning of the workday, whereas it tends to fill up later on. Location 7, as expected,

---

[1]We remark that the actual length of the prediction horizon n_h can eventually change in time, due to the shrinking of the remaining simulation time.

24

exhibits the opposite behavior. Both occupancy values are clearly outside the fixed desired occupancy, which would allow an efficient usage of the system, see Figs. 4 (a) and (c). The application of the proposed control strategy with a trade-off parameter set as $\gamma = 0.1$ leads to the results illustrated in Figs. 4 (b) and (d). It can be observed that, for both locations, the desired control performance in terms of the average value of state variables is attained. However, the effects of stochasticity cannot always be neglected. The average value of z_7, in fact, lays in a central region within the two prescribed bounds and, as a consequence, stochastic variations are also contained within those bounds. On the other hand, the control action tends to keep the average value of z_4 very close to the lower bound, implying that stochastic fluctuations lead to bound violations for about half of the trials.

This issue is successfully tackled in the next Section, where the results of the robust control strategy based on interval modeling defined in Section 4.4 are reported.

6.2. MPC control based on robust interval modeling

In this Section, numerical results obtained using the MPC control based on robust interval modeling, defined in Section 4.4, are reported. Similarly to the previous section, the whole control sequence over a time horizon of $n_h = 48$ time units is obtained by solving the optimization program (16), then only the current control input is applied to the system, the rest of the sequence is discarded, the system is simulated using Eqs. (3)-(4), the time index is updated and the control loop resumed.

Two parameters are important to assess the performance of the proposed control strategy: the trade-off parameter γ and the probability η, which in turn defines probabilistic bounds for the state variables (see Section 6.2). Besides the global

imbalance parameter f_E previously defined, a parameter representative of the control effort is considered, that is, the average number of bikes displaced for control purposes per time-step δ, computed as $f_R = J_T/n_h$.

The first assessment of the system performance consists of the evaluation of the two performance parameters as a function of the two control parameters. To this aim, the contour plots of Fig. 5, obtained performing 10 independent simulations for pairs of values of η and γ, selected over a two-dimensional grid spanning 20 values for each variable. The control effort is illustrated in Fig. 5(a). As intuition may suggest, directly from inspection of problem (16), larger values of γ imply a lower control effort. Parameter η has not, in general, a great influence on the control effort. However, its main role is to set a feasibility threshold on the control problem solution, and this threshold monotonically changes with η. Fixing a given value for η, in fact, implies fixing an estimate of the stochastic fluctuation of the state variables with a certain probability. Fixing a value for η, increasing γ implies the willingness to solve the control problem with a lower control effort. When the prescribed control effort is too small, problem (16) becomes unfeasible and the control objective cannot be attained. Increasing η, on the other hand, implies to consider greater stochastic fluctuations. Therefore, the limit for which the control problem is unfeasible is reached for lower values of γ. Figure 5(b), on the other hand, is representative of the rebalancing performance. It can be observed that, in general and as expected, a high control effort implies an excellent balancing performance. Focusing on the rebalancing parameter f_E alone, it can be observed that for intermediate values of the trade-off parameter (between about 0 and 6), f_E has a minimum for fixed γ, depending on η. This implies that there exists a range for the confidence interval of stochastic variabil-

26

ity that yields the best performance. This can be explained considering that, for very low values of η the control reduces to the control of the median value of the state variable, whereas, on the other hand, high values of η tend to overestimate the stochastic variability with the only effect of increasing the control effort and decreasing the control performance. For high values of γ, on the other hand, the performance with respect to η is monotonically decreasing. This is due to the fact that the main aim is to control the system assuming a high stochastic fluctuation and a low control effort, yielding unsatisfactory performance.

Figure 6 offers more elements of assessment and comparison with the previous control technique. For comparison purposes, Fig. 6(a) plots the two performance parameters, f_R vs. f_E. Each curve is plotted as a function of the trade-off parameter γ, which varies in logarithmic steps in the interval $\gamma \in [0.1, 100]$, for three fixed values of the confidence probability η: 0.01, 0.5, and 0.99. The following observations are in order: *i)* increasing the values of γ generally improves the system performance, both in terms of control effort and in terms of system balancing, however, this effect tend to saturate and further increases of γ become practically ineffective; and *ii)* the method based on robust interval modeling improves the performance of the control of the expected value for intermediate values of η, implying that there exists an *optimal value* for η, which guarantees the best improvement with respect to the control of the expected value. Figure 6(b) offers a direct insight on the occupancy state z_4 of location 4. Results are obtained in the same conditions of the control of the expected value (see Fig. 4(b)) and for $\eta = 0.5$. It can be observed that the control technique based on robust interval modeling outperforms the control technique based on expected values practically everywhere. However, a limited number of realizations of the simulations still

27

yield an occupancy status slightly out of the prescribed bounds. This is an effect of stochasticity, which can be hardly totally eradicated.

More insight on the rebalancing effort is offered in Fig. 7. Specifically, in Fig. 7(a), the trend of the number of bikes that travel in the system is plotted versus time. Namely, the number of bikes that are displaced by users' trips is displayed along with the corresponding number of bikes displaced for rebalancing purposes, for both the control on the expected value and the control based on robust interval modeling. Most importantly, it is observed that the rebalancing traffic is much less than the users' traffic, implying that the control is efficient. An observation of the opposite phenomena, on the other hand, would imply that almost every trip executed by a user should be compensated by a rebalancing trip, which is extremely costly and not in the spirit of a MOD system. A detailed illustration of the rebalancing trips in time is given in Fig. 7(b). There, it can be observed that the rebalancing activity using robust interval modeling is higher and has a greater variance than the control of the expected value, in order to compensate for the state variable stochasticity. Also, the rebalancing activity presents an important peak, corresponding to an intense rebalancing activity to compensate for the commuters' trips from peripheral to central locations at the start of the working day. Then, a lower and almost steady activity is realized, to compensate for the reduced number of trips. A slight increase toward the end of the working day tends to compensate for the traffic imbalance from the city center to the peripheral areas. The peak at the end of the day is less evident than that at the beginning of the day, since the system is more balanced by the predictive rebalancing activity throughout the day. It can be verified that the intra-day pattern of user trips is scarcely correlated with the number of rebalancing operations. This

28

counterintuitive observation implies that the rebalancing operations are not very dependent on the traffic, and this is due to the prediction capabilities of the model. The morning peak in the rebalancing operations, in fact, is present because the algorithm cannot be very accurate when it is initialized and starts the prediction. Figures 7(c) and 7(d) focus on the activity over the network links, that is, over the routes that connect one station to another. Figure 7(c) illustrates the cumulative distribution function (CDF) of the random variable $\mathscr{R}_{\text{link}}$, obtained summing all the rebalancing operations per link, over the entire time span and averaged over 100 independent simulations, for both the control of the expected value and that based on robust interval modeling. Interestingly, while the control based on robust interval modeling overall performs more rebalancing actions than that based on the expected value, these actions are concentrated on a fewer number of links. In fact, it can be verified that around the 40% of links experience a control activity close to zero in the robust control case. On the other hand, the control of the expected value performs rebalancing actions on almost all links of the system during one day. In conclusion, the control based on robust interval modeling is more efficient than that based on the expected value. Figure 7(d) plots the CDF of the random variable $\mathscr{D}_{\text{link}}$, obtained summing all the user trips per link, over the entire time span and averaged over 100 independent simulations. The CDF plot of Fig. 7(d) confirms that user traffic is much higher than the rebalancing activity and that it equally occurs over most of the link during the day.

Figure 8 focuses on the performance assessment with respect to local perturbations of the user demand, in space and time. The figures are obtained by selecting a random number ν of pairs of locations and time instants (i, t), and by imposing an instantaneous increment of the user demand $\lambda_i(t)$. Selected instantaneous

29

increments for this set of simulations are 10% and 20%. Figure 8(a) illustrates the result obtained with the control of the expected value, while Fig. 8(b) refers to the control based on robust interval modeling. As intuition may suggest, with both control strategies the imbalance parameter f_E tends to increase when the demand increase is more frequent in time and space. It can also be observed that the trend in the detriment of performance is almost linear with the number of perturbations. However, the performance attained with the control based on robust interval modeling is better than that attained through the control of the expected value.

The last set of simulations in Fig. 9 deal with a reduction of the traffic speed over a randomly selected fraction of links. In particular, the value of variable $q_{ij}(\delta)$ over the selected links is reduced by 20%, that is, $q_{ij}(\delta) \to 0.8 \, q_{ij}(\delta)$. It can be observed that, while the control of the expected value improves its performance with a slow down of a growing number of links (Fig. 9(a)), the performance of the control based on robust interval modeling is nearly not affected by such a variation (Fig. 9(b)). This is due to the fact that the control of the expected value is more prone to compensate for stochasticity, which is not explicitly accounted for, if it has more time available to implement the control strategy. On the other hand, the control based on robust interval modeling explicitly accounts for stochasticity, and the time available to compensate occurring variations is not relevant.

6.3. Investigation on seasonality patterns and the role of the time-horizon

In this section, we investigate on the periodicity of the system dynamics and the sensitivity of the performance of the control strategy with respect to the length of the MPC time horizon n_h. Here, we use a simulation time of a workweek, i.e., 5 consecutive days. Our simulations start at midnight on the first day and end at

30

midnight on the fifth day. To be consistent we the previous sections, and in view of the fact that no substantial differences in the system parameters have been revealed over different workdays, the input traffic parameters, $\lambda_i(t)$ and $p_{ij}(t)$ are repeated each day until the end of the simulation, whereas the rest of the quantities are simulated over a week through the stochastic model. The first simulation regards the effect of the MPC time horizon on the violation of the capacity constraints. In Fig. 10(a), we compare the outcome of two sets of Monte Carlo simulations, executed by applying the robust interval control method with an MPC time horizon of 2 and 12 hours, respectively. We plot the difference between the average values of the slack variables computed using the two time horizons. Such variables, we recall, quantify the number of violations of capacity constraints. We observe a slight trend whereby the 12-hours time horizon is advantageous over the 2-hours one, and such an advantage increases as long as the simulation time increases. However, the advantage is contained in the order of magnitude of fractions of vehicles per time unit. A more evident advantage of longer time-horizons resides in the magnitude of the control effort. Figure 10(b) illustrates the trend of the global control effort f_R, computed over Monte Carlo simulations, as a function of the MPC time horizon. In this case, the advantage in terms of control effort is apparent, since it monotonically decreases with increasing length of the the time horizon. We report that no relevant differences are observed applying the control of the nominal values, hence, the related results are not reported here for brevity. The most advantageous time horizon of 12 hours has been used to study the system behavior over a working week. Notably, Fig. 10(c) illustrates the distribution densities of the overall customer departures and overall rebalancing activity. We observe that the proposed model concentrates most of the rebalances after the

31

morning utilization peak, and overnight. Other times in the day involve a very moderate rebalancing action. This implies that efficient rebalancing can be performed with two different means: during the peak, with trucks, able to displace a high number of vehicles in a short time. Off-peak, on the other hand, the low-intensity rebalancing can be executed using smaller vehicles, like carts, or through incentives to users.

7. Conclusions

In this work, a novel control-oriented model able to describe the dynamics of MOD systems, either station-based or using floating locations, is introduced. The model enables analytical tractability, since it is described with dynamical equations in the state-space, using stochastic state variables. Reasonable simplifying assumptions lead to the definition of two MPC-based control strategies. First, a control of the expected value of the state variables is devised. Then, a robust control strategy that explicitly accounts for stochastic fluctuations via robust interval modeling is proposed. The model has been validated and its performance assessed on a real dataset of logged trips, made available by ToBike, one of the bike-sharing providers in Turin, Italy. Model parameters can be identified with relatively simple data processing operations. Both control methods lead to satisfactory results with a relatively low control effort. The slightly higher computational complexity of the robust controller based on interval modeling is fully repaid by a more efficient performance under different point of views. First, the control attains the expected results in most of the cases, despite the presence of important stochastic fluctuations. Second, even though the robust control usually displaces more vehicles than the control based on the expected values, those vehicles are moved

32

among a smaller set of routes, implying a control action that is more spatially concentrated. This obviously helps the design of rebalancing policies based on the displacement of large quantities of vehicles using trucks. Finally, the robustness of the proposed control methods to randomly applied perturbations and traffic slowdowns has been assessed, observing a gentle degradation of the performance, which makes the proposed methods promising for applications to real cases.

Future directions in our research contemplate the realization of optimized rebalancing strategies based on the rebalancing flows given by the solution of the optimization problems defined in this work. The typical rebalancing pattern obtained in this study exhibits a strong peak in the early morning and a less intense, and almost steady rebalancing activity throughout the day. This observation suggests that mixed rebalancing policies based on massive displacements in the first hours of the morning, e.g. operated by high-capacity trucks, followed by human-based rebalancing with less volume and frequency, e.g., achieved through incentives or gamification, may constitute viable and efficient strategies to make MOD systems effective, efficient, and available at any time of the day, increasing both the customer satisfaction and the provider revenues.

Conflict of Interest

The authors declare that they have no conflict of interest.

33

[1] R. Meddin, P. DeMaio, The bike-sharing world map, `http://www.bikesharingworld.com/`, 2018.

[2] Car2Go, `https://www.car2go.com/NA/en/press/`, accessed: 2018-02-28, ????

[3] P. Borgnat, P. Abry, P. Flandrin, C. Robardet, J.-B. Rouquier, E. Fleury, Shared bicycles in a city: A signal processing and data analysis perspective, Advances in Complex Systems 14 (03) (2011) 415–438.

[4] J. Froehlich, J. Neumann, N. Oliver, Measuring the pulse of the city through shared bicycle programs, Proceedings of UrbanSense08 (2008) 16–20.

[5] R. Nair, E. Miller-Hooks, R. C. Hampshire, A. Bušić, Large-scale vehicle sharing systems: analysis of Vélib', International Journal of Sustainable Transportation 7 (1) (2013) 85–106.

[6] M. Nourinejad, S. Zhu, S. Bahrami, M. J. Roorda, Vehicle relocation and staff rebalancing in one-way carsharing systems, Transportation Research Part E: Logistics and Transportation Review 81 (2015) 98–113.

[7] Z. Yang, J. Hu, Y. Shu, P. Cheng, J. Chen, T. Moscibroda, Mobility Modeling and Prediction in Bike-Sharing Systems, in: Proceedings of the 14th Annual International Conference on Mobile Systems, Applications, and Services, ACM, 165–178, 2016.

[8] E. O'Mahony, D. B. Shmoys, Data Analysis and Optimization for (Citi) Bike Sharing., in: AAAI, 687–694, 2015.

34

[9] M. Benchimol, P. Benchimol, B. Chappert, A. De La Taille, F. Laroche, F. Meunier, L. Robinet, Balancing the stations of a self service bike hire system, RAIRO-Operations Research 45 (1) (2011) 37–61.

[10] D. Chemla, F. Meunier, R. W. Calvo, Bike sharing systems: Solving the static rebalancing problem, Discrete Optimization 10 (2) (2013) 120–146.

[11] M. Rainer-Harbach, P. Papazek, B. Hu, G. R. Raidl, Balancing bicycle sharing systems: A variable neighborhood search approach, in: European Conference on Evolutionary Computation in Combinatorial Optimization, Springer, 121–132, 2013.

[12] M. Dell'Amico, E. Hadjicostantinou, M. Iori, S. Novellani, The bike sharing rebalancing problem: Mathematical formulations and benchmark instances, Omega 45 (2014) 7–19.

[13] M. Dell, M. Iori, S. Novellani, T. Stützle, et al., A destroy and repair algorithm for the bike sharing rebalancing problem, Computers & Operations Research 71 (2016) 149–162.

[14] G. Erdoğan, M. Battarra, R. W. Calvo, An exact algorithm for the static rebalancing problem arising in bicycle sharing systems, European Journal of Operational Research 245 (3) (2015) 667–679.

[15] A. Faghih-Imani, R. Hampshire, L. Marla, N. Eluru, An empirical analysis of bike sharing usage and rebalancing: Evidence from Barcelona and Seville, Transportation Research Part A: Policy and Practice 97 (2017) 177–191.

[16] T. Raviv, M. Tzur, I. A. Forma, Static repositioning in a bike-sharing system: models and solution approaches, EURO Journal on Transportation and Logistics 2 (3) (2013) 187–229.

[17] C. Contardo, C. Morency, L.-M. Rousseau, Balancing a dynamic public bike-sharing system, vol. 4, Cirrelt Montreal, 2012.

[18] J. Schuijbroek, R. C. Hampshire, W.-J. Van Hoeve, Inventory rebalancing and vehicle routing in bike sharing systems, European Journal of Operational Research 257 (3) (2017) 992–1004.

[19] D. Chemla, F. Meunier, T. Pradeau, R. W. Calvo, H. Yahiaoui, Self-service bike sharing systems: simulation, repositioning, Tech. Rep., pricing. Tech. Rep. hal-00824078, Centre dEnseignement et de Recherche en Mathématiques et Calcul Scientifique (CERMICS), 2013.

[20] J. Pfrommer, J. Warrington, G. Schildbach, M. Morari, Dynamic vehicle redistribution and online price incentives in shared mobility systems, IEEE Transactions on Intelligent Transportation Systems 15 (4) (2014) 1567–1578.

[21] A. Singla, M. Santoni, G. Bartók, P. Mukerji, M. Meenen, A. Krause, Incentivizing Users for Balancing Bike Sharing Systems., in: AAAI, 723–729, 2015.

[22] C. Fricker, N. Gast, Incentives and redistribution in homogeneous bike-sharing systems with stations of finite capacity, Euro journal on transportation and logistics 5 (3) (2016) 261–291.

36

[23] G. C. Calafiore, F. Portigliotti, A. Rizzo, A Network Model for an Urban Bike Sharing System, IFAC-PapersOnLine 50 (1) (2017) 15633–15638.

[24] G. C. Calafiore, F. Portigliotti, A. Rizzo, C. Novara, A flow optimization approach for the rebalancing of mobility on demand systems, in: IEEE Conference on Decision and Control, 1–6, 2017.

[25] D. Zeng, J. Xu, J. Gu, L. Liu, G. Xu, Short term traffic flow prediction based on online learning SVR, in: Power Electronics and Intelligent Transportation System, 2008. PEITS'08. Workshop on, IEEE, 616–620, 2008.

[26] L. Zhao, F.-Y. Wang, Short-term traffic flow prediction based on ratio-median lengths of intervals two-factors high-order fuzzy time series, in: Vehicular Electronics and Safety, 2007. ICVES. IEEE International Conference on, IEEE, 1–7, 2007.

[27] I. Kaysi, M. E. Ben-Akiva, H. Koutsopoulos, An integrated approach to vehicle routing and congestion prediction for real-time driver guidance, vol. 1408, Transportation Research Board, 1993.

[28] G. Calafiore, C. Bongiorno, A. Rizzo, A control-oriented model for mobility on demand systems, in: "Proceedings of the 57th IEEE Conference on Decision and Control, CDC 2018", 2018.

[29] E. F. Camacho, C. B. Alba, Model predictive control, Springer Science & Business Media, 2013.

[30] S. Lloyd, Least squares quantization in PCM, IEEE transactions on information theory 28 (2) (1982) 129–137.

[31] J. P. Snyder, Flattening the earth: two thousand years of map projections, University of Chicago Press, 1997.

[32] S. Weikl, K. Bogenberger, Relocation strategies and algorithms for free-floating car sharing systems, IEEE Intelligent Transportation Systems Magazine 5 (4) (2013) 100–111.

[33] S. Gupta, A. Agrawal, K. Gopalakrishnan, P. Narayanan, Deep learning with limited numerical precision, in: International Conference on Machine Learning, 1737–1746, 2015.
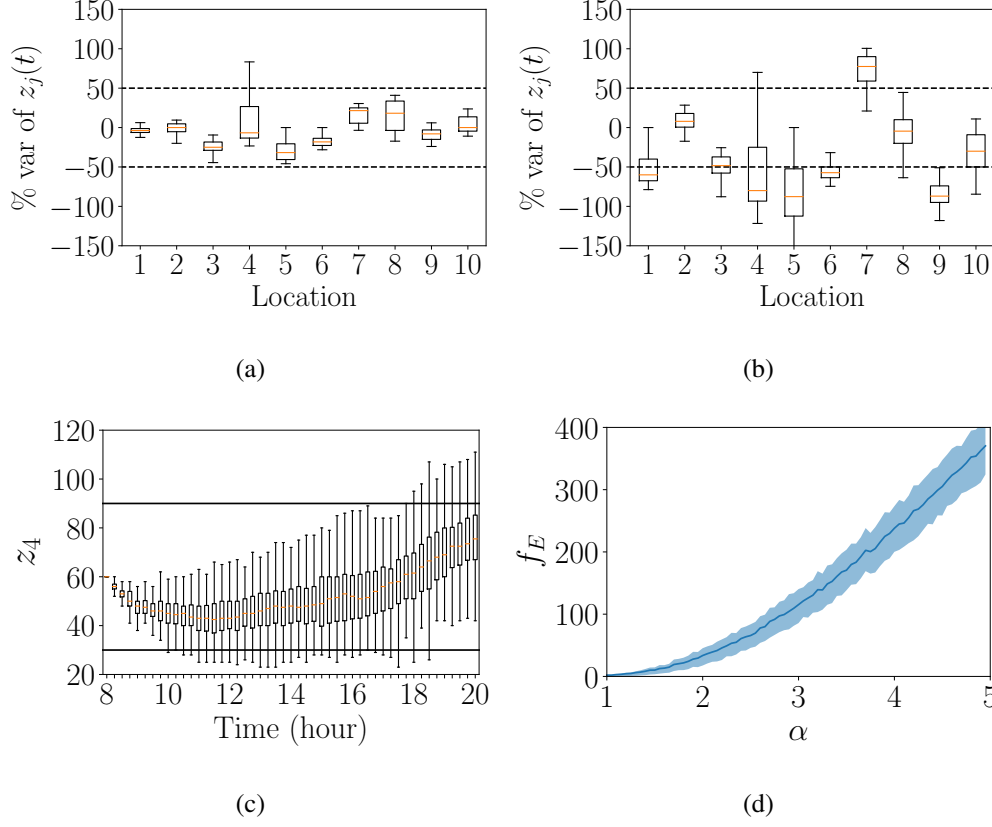
Figure 3: Outcome of an open-loop stress test on the departure rates $\lambda_i(t)$ performed over 100 independent daily Monte Carlo simulations, without the application of control actions. (a) percentage variations, with respect to their initial values $z_i(0)$, of the number of bikes at considered locations, with the original departure rates $\lambda_i(t)$ estimated from logged trip data; (b) same as (a), under the stress test with departures rate proportionally increased by a stress factor $\alpha = 4$; (c) detailed trend, for zone 4, of the state variable $z_4(t)$ with original departure rates. Boxes represent the 25-75 percentile range, whiskers represent extreme values, and orange lines the median ones. Continuous horizontal lines indicate the location capacity limits. In (d), trend of the global imbalance parameter f_E as a function of the stress factor α. The blue line indicates the mean value, the band indicates the 25-75 percentile range.
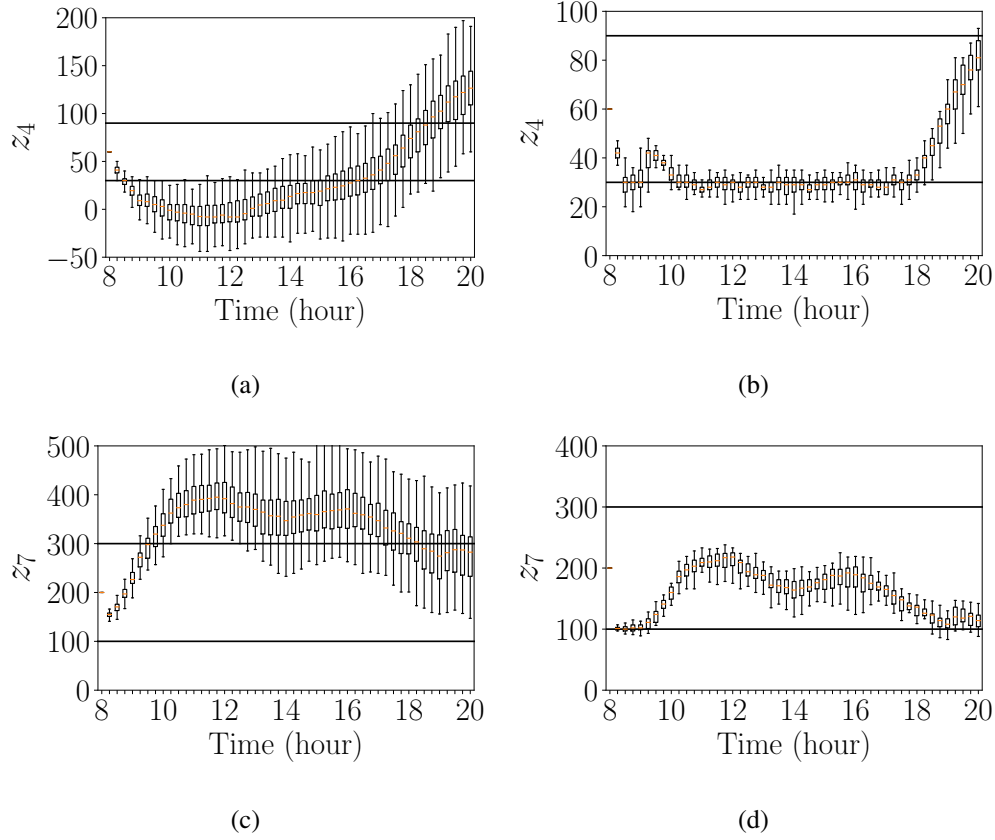
Figure 4: Monte Carlo simulations of the ToBike system in a 12 hours time interval, from 8AM to 8PM. Results are obtained over 100 independent simulations. (a),(b) occupancy for location 4 and location 7, respectively, in uncontrolled mode. (c),(d) simulation for with control on the expected values for the same locations. The continuous upper and lower lines in each plot indicate the desired upper and lower capacity bound for the locations. Boxes represent the $25 - 75$ percentile range, whiskers represent extreme values, and orange lines the median ones.
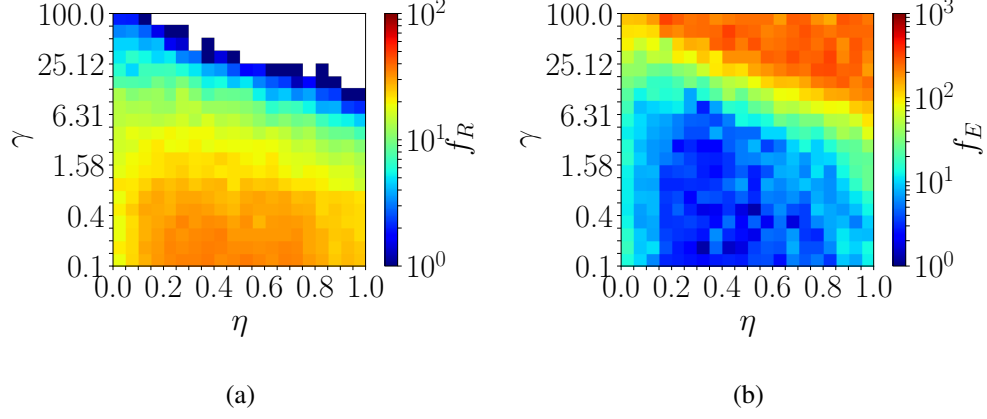
Figure 5: Performance of the MPC control based on robust interval modeling: (*a*) global control effort as a function of η and γ; (*b*) global imbalance indicator for the same parameters. Each value is a mean of 10 independent simulations with a robust control. White regions in panel (a) corresponds to unfeasible solutions of the optimization problem.
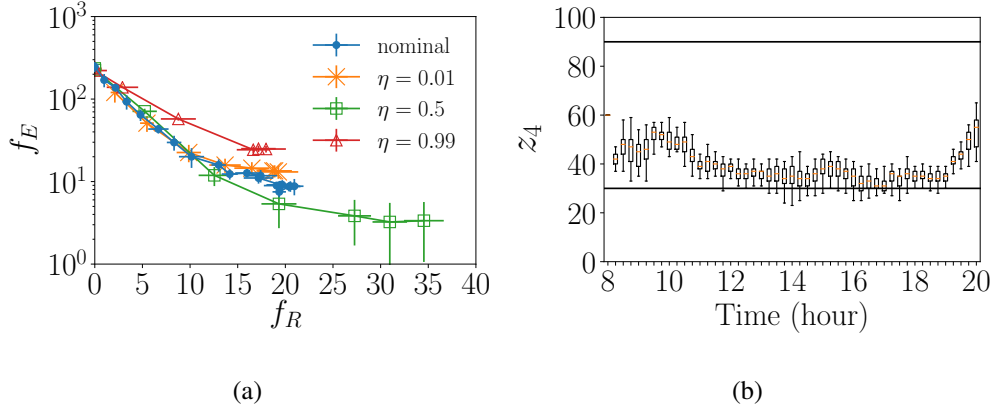

Figure 6: Performance assessment and comparison of the control technique based on robust interval modeling. In (a), performance curves f_E vs. f_R, plotted for a logarithmic interval of $\gamma \in [0.1, 100]$, and for $\eta = 0.01, 0.5, 0.99$. The blue plot corresponds to the performance of the control method based on the expected value, described in Section 6.1. In (b), trend of the occupancy state z_4 over a 12 hours interval, from 8AM to 8PM. Results are obtained in the same condition of the control of the expected value and setting $\eta = 0.5$.
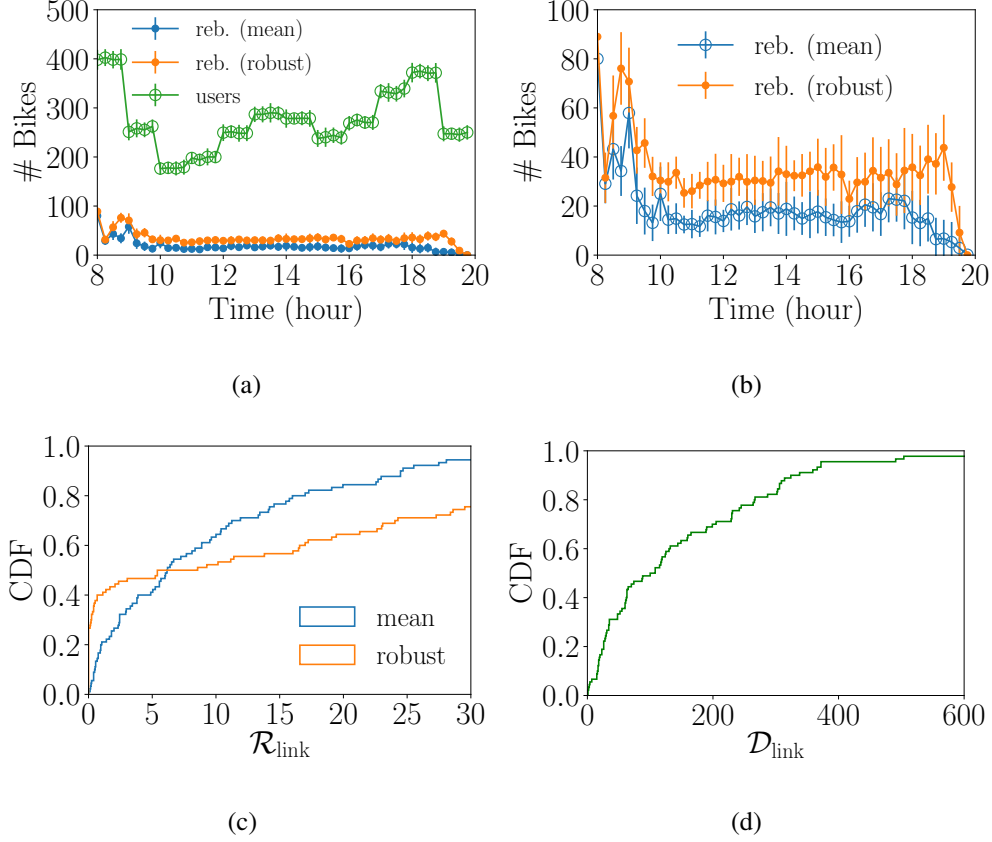
(a)

(b)

(c)

(d)

Figure 7: Control performance assessment performed over 100 independent simulations, for $\gamma = 0.1$ and $\eta = 0.5$. In panel (a), the green line illustrates the average number of user trips over time during a whole day, from 8AM to 8PM. The orange and the blue lines illustrate the average number of rebalancing operations during the same day, using the control of the expected value and that based on robust interval training, respectively. Panel (b) illustrates the control activity only, where the vertical bars indicate one standard deviation. Panel (c) illustrates the CDF of the random variable $\mathscr{R}_{\text{link}}$, representative of the control activities over the network links. Panel (d) illustrates the CDF of the random variable $\mathscr{D}_{\text{link}}$, representative of the user trips over the network links.
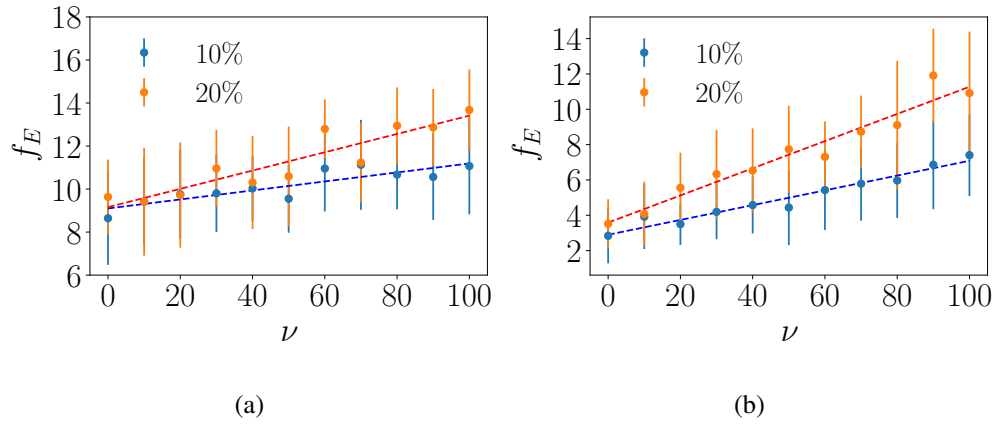
(a)   (b)

Figure 8: Control performance under instantaneous variations of user demand in time and space. The figures show the effect on global imbalance parameter (f_E) caused by an instantaneous percentage increment of the departure rate that affect a randomly selected subset of size ν consisting of pairs of stations and time instants. Blue dots refer to a demand increment of 10%, orange dots refer to an increment of 20%. Results are obtained averaging over 30 independent simulations. Dots indicate the mean, bars indicate one standard deviation, the dotted line is a linear fit. Panel (a) refers to the control of the expected value, panel (b) to the control based on robust interval modeling.
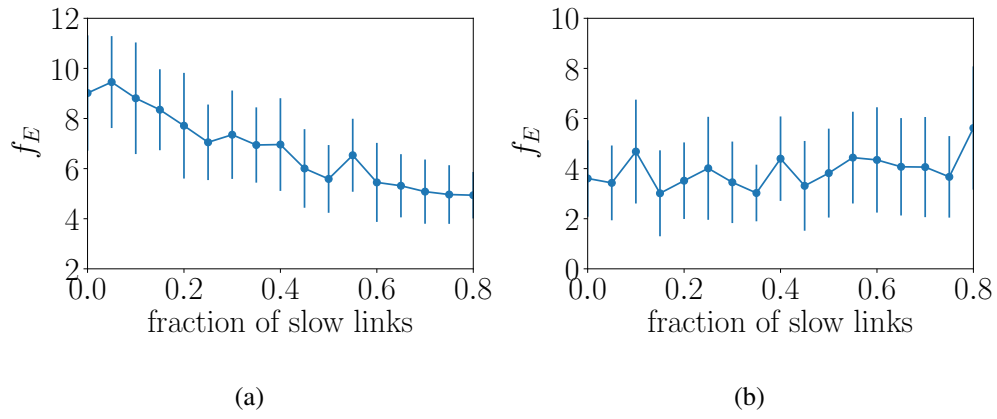
Figure 9: Effects of a local reduction of 20% of the link speed imposed to a random fraction of links. In panel (a), results are obtained via the application of the control of the expected value; in panel (b), via the application of the control with robust interval modeling. Each point is obtained as the average of 30 independent Monte Carlo simulations. Bars indicate one standard deviation.

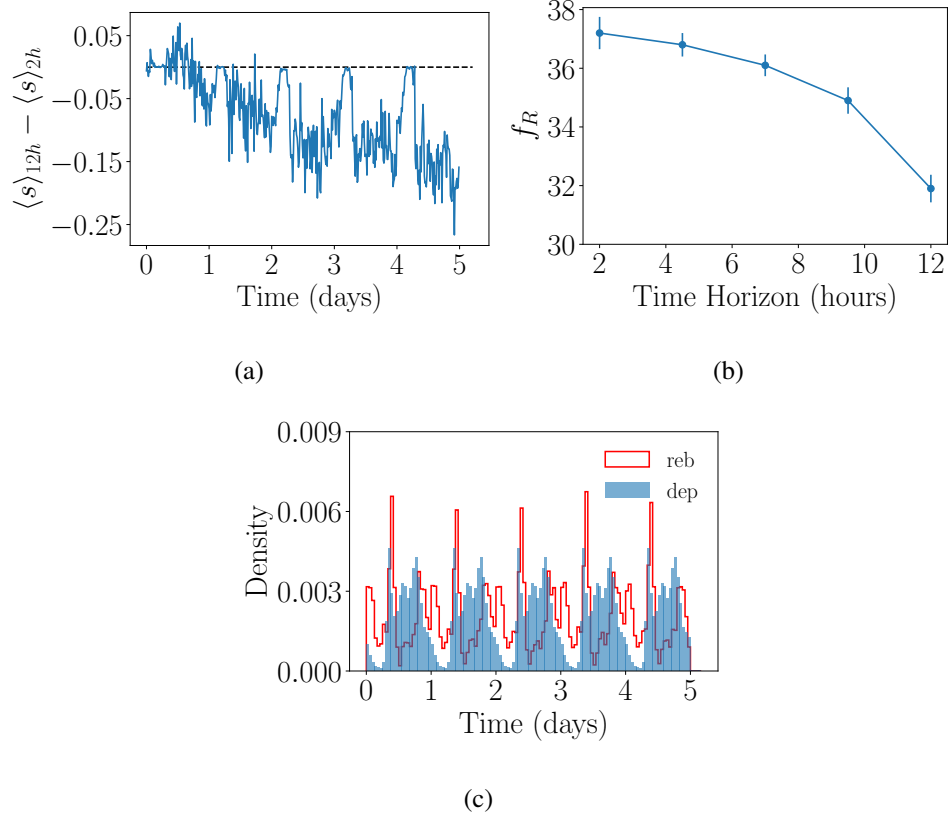(a)   (b)

(c)

Figure 10: System characterization with respect to the MPC time horizon and weekly periodicity. Results are averaged over 10 independent Monte Carlo simulations. (a) Difference between the overall violation of the capacity constraints with a 2- and 12-hour time horizon; (b) Global control effort f_R as a function of the time-horizon (the bands quantifies the 95% confidence interval); (c) Distribution of the rebalancing operations (red) and expected number of departures (blue) as a function of time, along a workweek, using a 12-hours time horizon.